Fracture toughness and morphology study of ternary blends of epoxy, poly(ether sulfone) and acrylonitrile–butadiene rubber

S. Horiuchi*, A. C. Street, T. Ougizawa and T. Kitano
National Institute of Materials and Chemical Research, 1-1 Higashi, Tsukuba, Ibaraki 305, Japan
(Received 18 February 1994; revised 4 April 1994)

An epoxy resin based on diglycidyl ether of bisphenol A has been modified with poly(ether sulfone) (PES) and poly(acrylonitrile-*co*-butadiene) rubber (NBR) and cured with 4,4′-diaminodiphenylsulfone. The fracture behaviour of the ternary blend was examined using a fracture mechanics approach. Depending on the combination of PES and NBR, two distinct morphological states were shown, and the fracture behaviour varied from brittle to ductile with changing morphology. From fracture surface observations by scanning electron microscopy, the ternary blends that showed ductile fracture behaviour have a phase-inverted morphology in which the NBR-rich phase formed a continuous matrix, the epoxy-rich phase formed particles and the PES-rich phase also formed particles around the epoxy particles. Dynamic mechanical thermal analysis revealed that the ternary blends exhibited high T_g, as high as the T_g of the unmodified epoxy resin.

(Keywords: ternary epoxy blends; mechanical properties; morphology)

INTRODUCTION

Epoxy resins are used extensively in areas where their stiffness, temperature performance and solvent resistance are required. They are, therefore, one of the principal materials for coatings, adhesives, electrical laminates and fibre-reinforced structural component applications. The resin's desirable properties stem from the high crosslink density that develops on cure. However, the fully cured resin cannot absorb energy under stress, and hence is of a brittle nature. Thus tremendous effort has been, and is currently being, focused on improving the toughness of epoxy resins.

The most successful and most well established method of increasing their toughness is to incorporate a second phase of dispersed rubbery particles into the crosslinked polymers[1,2]. Addition of rubbery materials to epoxy resins has been shown to enhance their fracture toughness while lowering their glass transition temperature (T_g) and thermal and solvent stability. This limits the number of high-performance applications such as aerospace, advanced marine, transportation and building construction. Recently, high-performance thermoplastics have been used to toughen epoxy resins[3–9]. Owing to the high modulus and high T_g of these thermoplastics, the modulus and T_g of the modified epoxy resin can reach or even surpass those of the neat epoxy resin. The thermoplastic modification of epoxy resins provides a solution to the embrittlement, with minimal loss in other desirable properties. It has also been shown that the thermoplastic-modified epoxies exhibit various types of morphology, depending crucially on their backbone structure, molecular weight and the end-group chemistry of the thermoplastics, and through morphological control desirable fracture toughness properties can be achieved[6]. However, the difficulty of controlling morphology limits the further improvement of toughness in thermosetting resins.

There seem to be few works on ternary blends of thermoplastics and rubber with epoxy. Pearson and Yee[10] have investigated ternary blends of poly(phenylene oxide)/styrene–butadiene–styrene triblock copolymer (PPO/SBS) and poly(phenylene oxide)/carboxyl-terminated butadiene–acrylonitrile rubber (PPO/CTBN) with epoxy. Although the addition of rubber results in an increase in fracture toughness in PPO-modified binary epoxies, the effect on fracture toughness is no greater than that with CTBN alone. This implies that the interaction between rubber and thermoplastic does not work additively on fracture toughness. A group at Fudan University[11] has studied the toughening of epoxy by a copolymer of poly(ether sulfone) (PES) and n-butyl acrylate. A blend of PES and the copolymer as a modifier for epoxy resulted in an increase in fracture toughness.

The objective of the present work was to evaluate the effect of the combination of rubber and ductile thermoplastic on the fracture toughness of epoxy resin, and to examine the morphology changes in such systems. More specifically, the effect of adding poly(acrylonitrile-*co*-butadiene) rubber (NBR) to PES/epoxy blend has been investigated.

* To whom correspondence should be addressed

0032-3861/94/24/5283–10

EXPERIMENTAL

Materials

All the materials used throughout this work were from commercial sources and were used as received. The epoxy resin employed was Epicote 828, comprising bisphenol A and epichlorohydrin, as supplied by Shell Chemical Co., cured with 4,4'-diaminodiphenylsulfone (DDS). This resin had an epoxy equivalent weight of 188.5 g mol^{-1}. The thermoplastic was poly(ether sulfone) (PES), supplied by ICI (Victrex 5003P, $M_n = 25000$). The rubber used here was nitrile–butadiene rubber, NBR41, with a bound acrylonitrile content of 41%, as supplied by Japan Synthetic Rubber Co.

Curing procedure

The rubber and epoxy components were mixed in dichloromethane/methanol 90/10 v/v, and the solution was stirred for approximately 30 min to achieve dissolution. The thermoplastic was dissolved in the same mixed solvent combination, and this solution was filtered through glass wool into the epoxy/rubber mixture. It was then heated to remove excess solvent and then DDS was added to the mixture at 80% stoichiometrically. This was then poured into a preheated mould at 145°C. The sample was degassed *in vacuo* at 145°C for 30 min in an open mould, cured at 180°C in air at atmospheric pressure, and allowed to come to room temperature. *Table 1* lists the formulations evaluated in this study.

Fracture toughness measurements

The fracture toughness was measured using a single-edge-notched specimen (5.0 mm × 10 mm × 60 mm) in a three-point bending geometry by applying either linear elastic fracture mechanics or non-linear elastic fracture mechanics. These specimens were cut out from the moulded samples, a sharp notch was machined in each specimen and a natural crack was generated by tapping a new razor blade placed in the notch. Before use, the razor blade was cooled in liquid nitrogen, which facilitated the propagation of a sharp crack in front of the tip of the razor blade.

For the materials showing brittle fracture behaviour, linear elastic fracture mechanics was used in accordance with the European Structural Integrity Society[12]; the critical stress intensity factor, K_{Ic}, and the critical strain energy release rate, G_{Ic}, for the initiation of crack growth were determined using a single-edge-notched specimen in a three-point bending geometry. The results given are the average of at least five test specimens. The tests were performed on a Shimazu testing machine at a constant crosshead speed of 0.5 mm min^{-1} at room temperature. K_{Ic} was calculated from:

$$K_{Ic} = Y \frac{3PSa^{1/2}}{2BW^2} \tag{1}$$

Here P is the critical load for crack propagation, S is the length of the span, a is the crack length, B is the thickness, W is the width and Y is the non-dimensional shape factor, given by:

$$Y = \frac{1.99 - (a/W)(1-a/W)[2.15 - 3.93a/W + 2.7(a/W)^2]}{(1 + 2a/W)(1-a/W)^{3/2}} \tag{2}$$

G_{Ic} values were determined using the following relationship:

$$G_{Ic} = \frac{U}{BW\phi} \tag{3}$$

Here U is the stored elastic energy, determined from the area under the load *versus* displacement curve, and the energy calibration factor, ϕ, is defined as:

$$\phi = C\left(\frac{dc}{d(a/W)}\right)^{-1} \tag{4}$$

and may be evaluated either from measuring the compliance C as a function of crack length or more readily from published tables. In the present work the values of ϕ were taken from the table in the testing protocol of the European Structural Integrity Society[12].

To characterize the ductile fracture toughness behaviour, the multi-specimen R-curve method was used in accordance with the recommended procedure for establishing J_{Ic} outlined by ASTM[13]. More specifically, a number of cracked three-point bend specimens were loaded to various displacements, producing different amounts of crack extension, Δa, and then unloaded. Extension Δa was determined by marking crack growth with a permeable dye that was injected into the specimen notch before testing[14]. The value of J for each specimen was determined from the area under its load *versus* displacement curve and the relationship given by:

$$J = \frac{2U}{B(W - a)} \tag{5}$$

The R-curve (J vs. Δa) was then constructed and J_{Ic} was taken by extrapolating the line to the point at which Δa was zero.

Table 1 List of formulations for this study

Designation	Epoxy (g)	DDS (g)	PES (g)	NBR (g)
Epoxy	79	21	0	0
N5	79	21	0	5
N10	79	21	0	10
N15	79	21	0	15
P5	79	21	5	0
P10	79	21	10	0
P30	79	21	30	0
P5N5	79	21	5	5
P5N10	79	21	5	10
P10N5	79	21	10	5
P10N10	79	21	10	10
P15N5	79	21	15	5
P15N10	79	21	15	10
P20N5	79	21	20	5
P20N10	79	21	20	10

Dynamic mechanical thermal analysis

Dynamic mechanical measurements were carried out on a Rheovibron model DOV EA dynamic viscoelastometer (Tokyo Baldwin Co., Japan), with temperature scanned from −150 to +250°C. The frequency used was 11 Hz and the heating rate was 2.0°C min^{-1}. T_g values refer to the maximum in tan δ.

Morphological observation

Scanning electron microscopy (SEM) and transmittance optical microscopy (TOM) were used to observe the morphology of the cured blends. For morphological

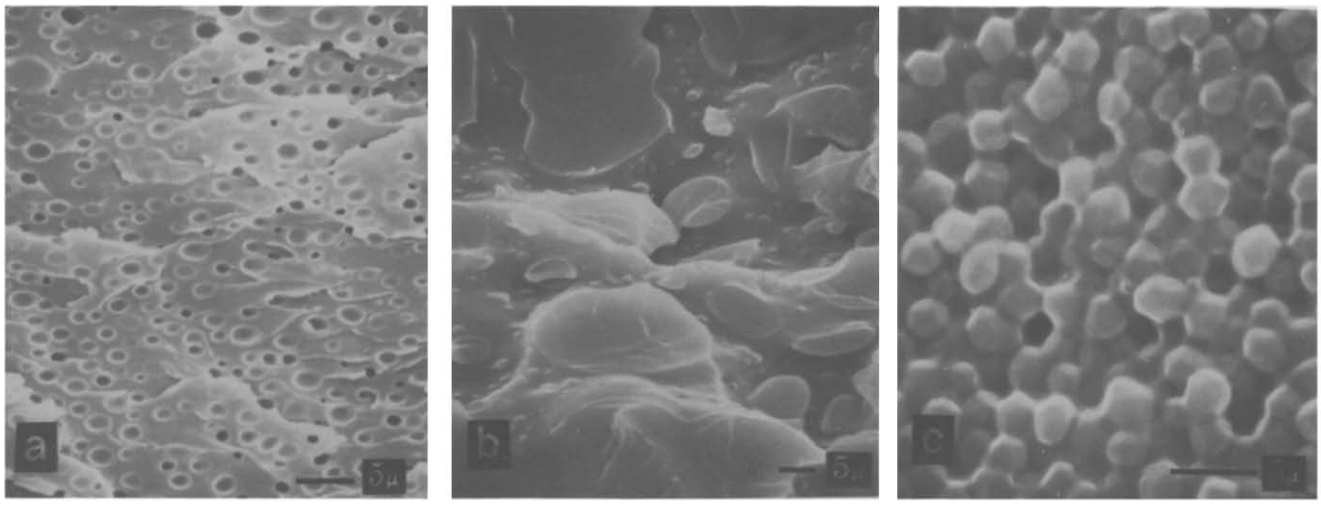

Figure 1 SEM micrographs of fracture surfaces, illustrating the effect of varying the concentration of NBR on the morphology of NBR-modified binary epoxies: (a) 5 phr NBR; (b) 10 phr NBR; (c) 15 phr NBR

observation by SEM, cured plaques were fractured under cryogenic conditions using liquid nitrogen and then coated with gold to reduce any charge build-up. To detect the crack tip deformation, the load samples were observed using SEM.

TOM observations were also carried out to observe the morphology. The specimens for TOM observations were prepared by microtoming of the cured blends with a glass knife at room temperature.

Energy-dispersive spectroscopy

In order to identify the location of the PES phase in the ternary blend of epoxy/poly(ether sulfone)/rubber, an energy-dispersive analyser (Phillips EDAX ECON) attached to an SEM (Akashi ISI-DS 130 Dual Stage) was used. This technique has recently been used to examine the morphology in a blend of poly(ether sulfone) and bismaleimide resin[15]. The bombardment of incident electrons on the sample surface leads to back-scattering of X-rays, the energies of which are analysed. Each energy is characteristic of the element from which it came, and thus, in the case of the ternary blends, the presence of sulfur in the poly(ether sulfone) backbone allows the thermoplastic-rich phase to be identified. (Although the curing agent used, DDS, also contains sulfur, the concentration of the curing agent was much less than that of the thermoplastic.) Prior to analysis, the samples were carbon-coated using a JEOL JEE 4B vacuum evaporator.

RESULTS AND DISCUSSION

Morphology

Morphological features of the NBR/epoxy and PES/epoxy binary systems and NBR/PES/epoxy ternary system can be found in the SEM and OTM micrographs.

The SEM micrographs of the NBR/epoxy binary blends are shown in *Figure 1*. Such micrographs show a tendency towards formation of morphological features in modified epoxies with increase of rubber content. The modified epoxy containing 5 phr NBR (*Figure 1a*) shows the typical particulate morphology in which NBR-rich particles are dispersed in the epoxy-rich phase. The

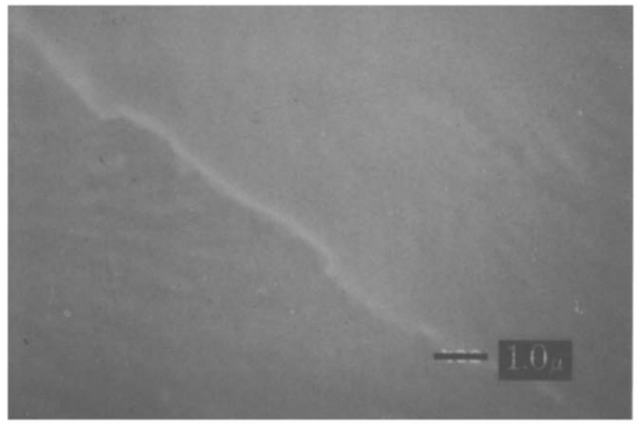

Figure 2 SEM micrograph of 30 phr PES-modified epoxy showing a featureless fracture surface

Figure 3 SEM micrograph of P10N5 ternary epoxy's fracture surface illustrating the particulate morphology

10 phr NBR-modified epoxy shows a relatively rough fracture surface, as shown in *Figure 1b*, and thus it is difficult to identify morphological features. Modified epoxies containing more than 15 phr of NBR show phase-inverted nature in which the NBR-rich phase is formed as a continuous phase, as shown in *Figure 1c*.

In contrast, PES-modified epoxies showed no surface features, as shown in *Figure 2*. Previous detailed studies have shown that the morphology of epoxy/thermoplastic blends can be tailored by varying the thermoplastic concentration, thermoplastic molecular weight, thermoplastic backbone structure, or reactive end-group concentration[6]. By changing these parameters, homogeneous, particulate, co-continuous and phase-inverted type morphologies can be achieved. Within our observations of fracture surfaces in PES-modified epoxies, no morphological features were exhibited within the composition range in this work, which indicates that PES and epoxy are completely miscible and form a single phase. Further evidence for miscibility was obtained by d.m.t.a., shown later.

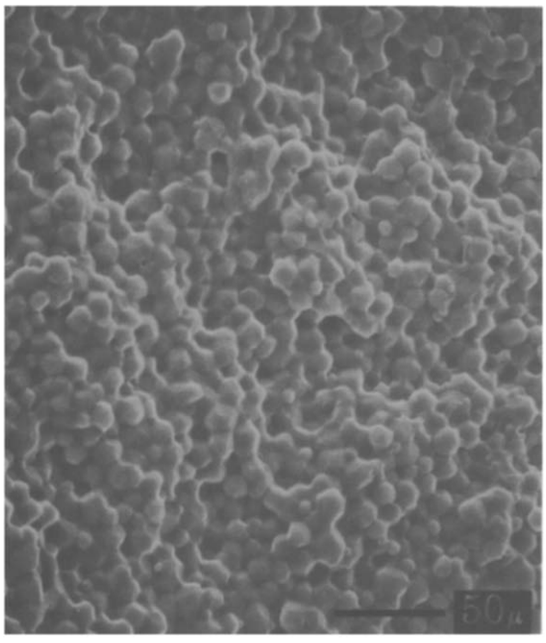

Figure 4 SEM micrograph of P5N10 ternary epoxy's fracture surface illustrating the phase-inverted morphology

In the NBR/PES/epoxy ternary system, two distinct types of morphologies could be found, as shown in the SEM micrographs in *Figures 3* and *4*. The micrograph in *Figure 3* shows clear phase separation in which the particles aggregate and form spherical domains ranging in size from 30 to 100 μm. The micrograph in *Figure 4* shows another type of morphology in which a large number of globules with a relatively uniform diameter are seen. With respect to the volume fraction of each component of the ternary blends, the globules are assumed to consist mainly of crosslinked epoxies, which indicates that phase inversion has occurred and that epoxy-rich spherical domains are dispersed regularly in the matrix. By careful observations of the fracture surface at high magnification in SEM, as shown in *Figure 5a*, it has been found that particles smaller than the epoxy-rich ones exist and that this system is three-phase. In particular, the micrograph in *Figure 5b* shows cavities of the particles, which indicates that small particles tend to exist around the epoxy-rich particles. The matrix and the smaller particles can be consistently referred to as either NBR-rich or PES-rich phase. *Figure 6* shows TOM micrographs at the same magnification of the phase-inverted morphology with a different combination of PES and NBR contents. It is obvious that the size of the epoxy-rich particles in each formulation is different. The average particle size increases with decrease of weight per cent incorporation of NBR and is much bigger than that observed in the NBR-modified binary system (N15).

Figure 7 shows the sulfur distribution line profile obtained from EDAX for the morphology shown in *Figure 3*. The (barely visible) horizontal line through the

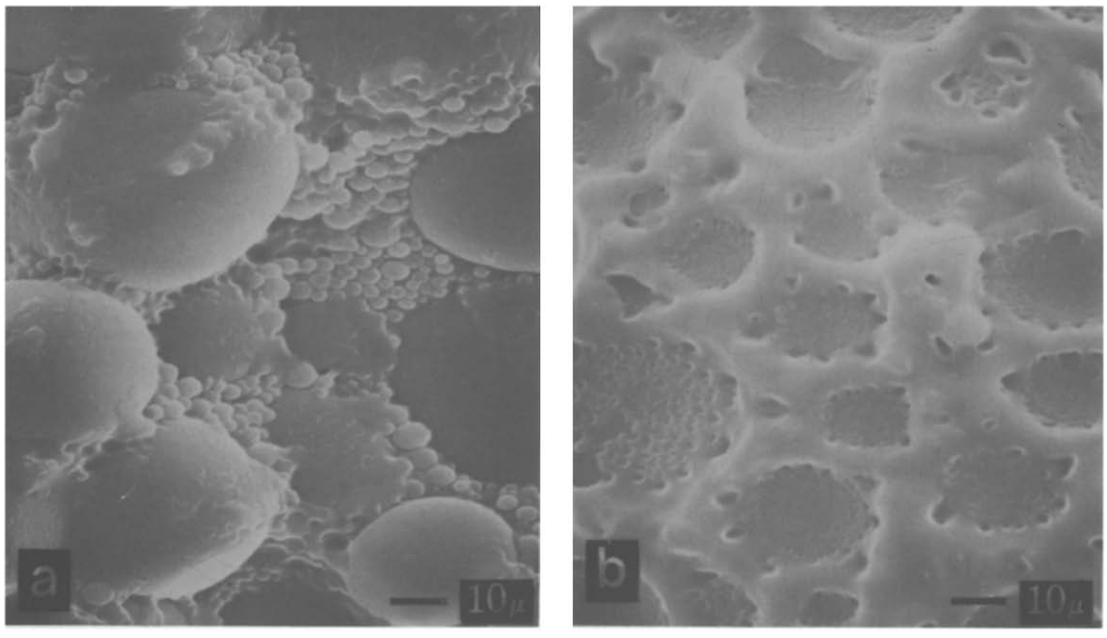

Figure 5 SEM micrograph illustrating: (a) small particles around epoxy-rich particles in fracture surface of P5N5 ternary epoxy; (b) cavities corresponding to the small particles in fracture surface of P15N10 ternary epoxy

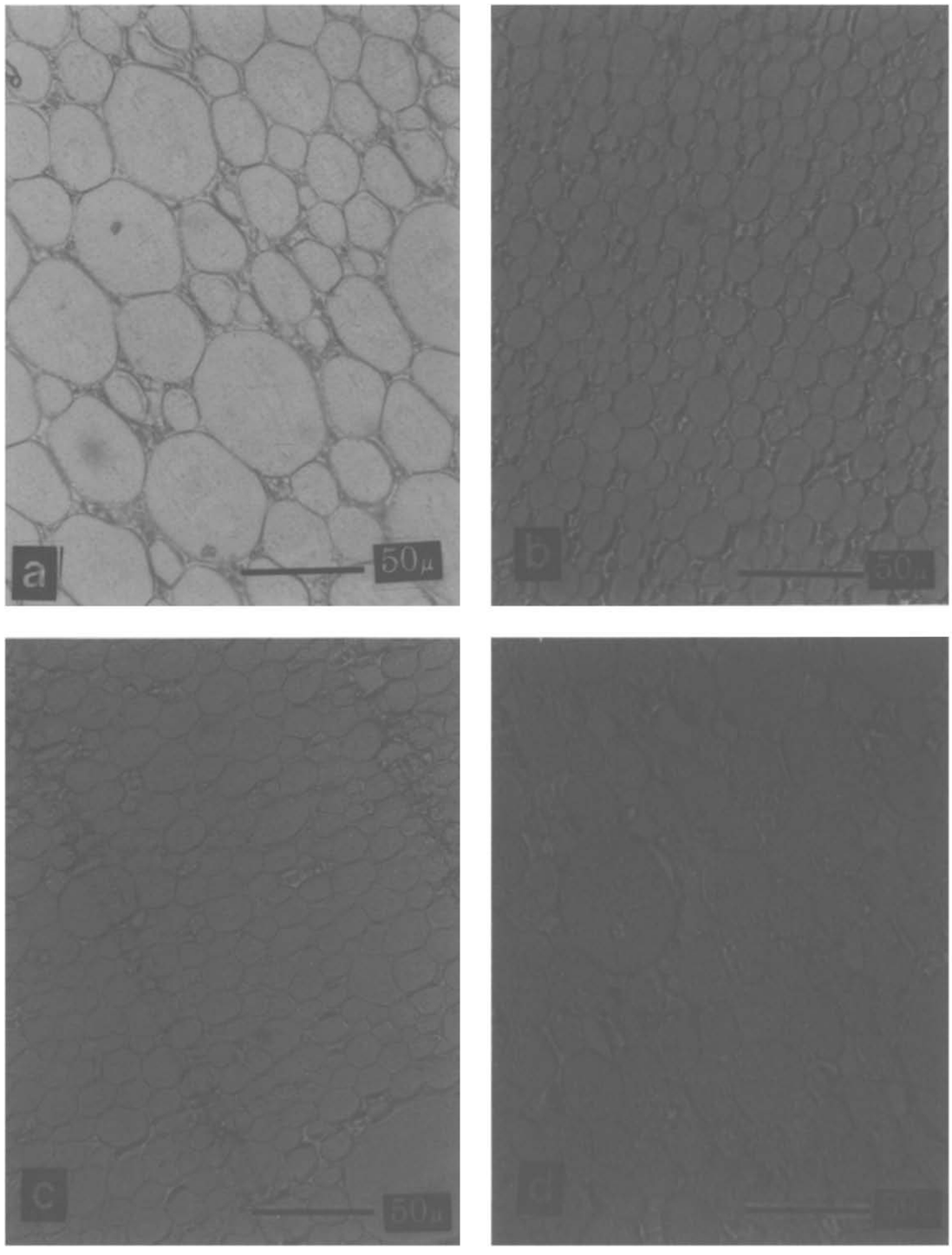

Figure 6 TOM micrographs of phase-inverted morphology at ×375 magnification: (a) P5N5 (incorporation of NBR is 4.5 wt%); (b) P5N10 (8.7 wt%); (c) P10N10 (8.3 wt%); (d) P15N10 (8.0 wt%). The particle size increases with decrease of weight per cent incorporation of NBR

centre of the micrograph shows the axis along which the sulfur distribution was measured. As can be seen from the distribution profile (also barely visible), the featureless areas of the fracture surface are rich in sulfur and therefore correspond to the PES-rich phase, and the areas that are poor in sulfur correspond to NBR-rich phase.

Fracture toughness

Typical load–displacement curves obtained in this study are shown in *Figure 8*. Curve A in *Figure 8* represents brittle unstable crack growth, which is a linear diagram with an abrupt drop of load to zero at the instant of crack growth initiation. Curve B represents brittle unstable crack growth, which is also a linear diagram, but crack growth is in stick–slip manner; and curve C represents ductile stable crack growth in which cracking is continuous and stable.

In this study, the NBR-modified binary epoxies containing 5 and 10 phr and all PES-modified binary epoxies exhibited brittle fracture behaviour, with the load

versus displacement curve of type A. In the ternary formulations, the systems that have particulate morphology as shown in *Figure 3* exhibited brittle fracture behaviour with the curve of type B, and the formulations that have the phase-inverted morphology exhibited ductile fracture behaviour with the curve of type C. The NBR-modified binary epoxies containing more than 15 phr of NBR also showed ductile fracture behaviour. *Table 2* lists the K_{Ic} fracture toughness values and G_{Ic} fracture energy values for the systems that showed brittle fracture behaviour. As is well known in the earlier literature[1,2], the addition of NBR rubber results in the expected increase in fracture toughness; furthermore, the addition of PES also results in the increase in fracture toughness[3].

In the ternary formulations that have the particulate morphology, the load–displacement curve was linear and, after crack growth initiation, a crack propagated in stick–slip manner as shown in *Figure 8*. By observation of the fracture surface as shown in *Figure 3*, it has been found that the crack propagates with an abrupt drop through the matrix and then stops at the rubber domain surface and deviates from its path. Such a deviation

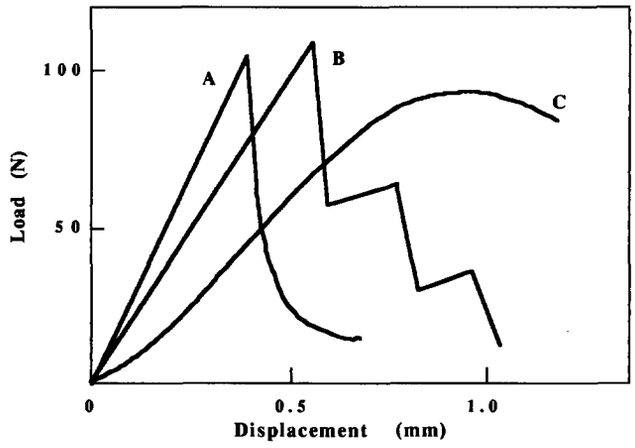

Figure 8 Typical load–displacement curves of fracture toughness measurements illustrating: (A) brittle unstable crack growth; (B) brittle unstable crack growth and crack propagation in stick–slip manner; (C) ductile stable crack growth

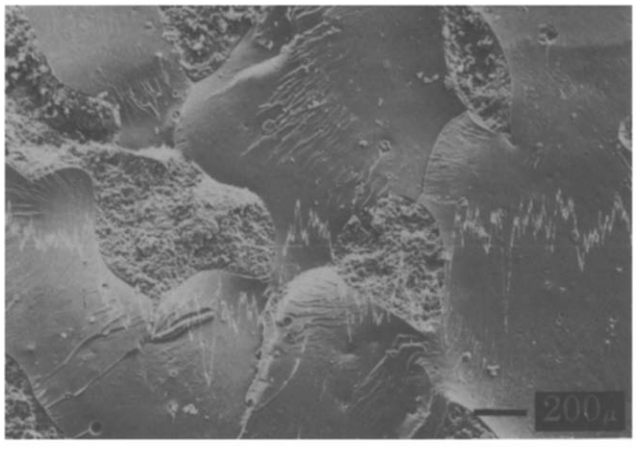

Figure 7 Sulfur line profile using energy-dispersive spectroscopy to identify the location of PES in particulate morphology of the ternary blend

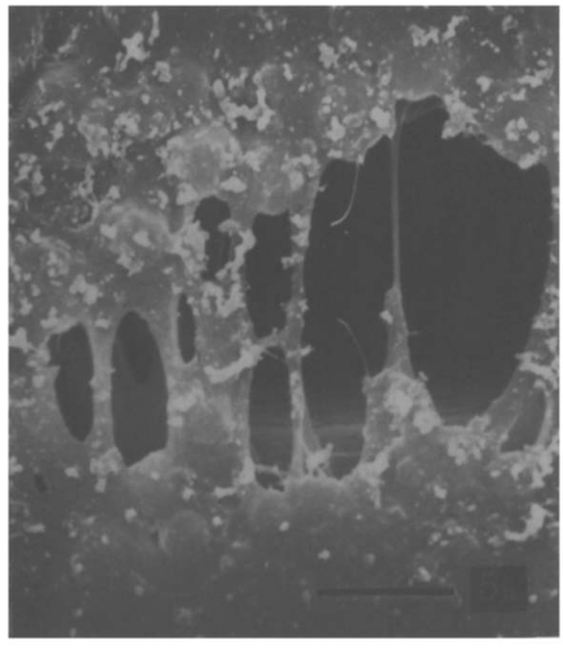

Figure 9 SEM micrograph showing the deformation at the crack front in three-point bend specimen

Table 2 Mechanical and morphological properties of modified epoxies

Loading level (phr)						
PES	NBR	K_{Ic} (MN m^{-2})	G_{Ic} (kJ m^{-2})	J_{Ic} (kJ m^{-2})	Fracture behaviour	Morphology
0	0	0.73	0.15	0.16	Brittle	Homogeneous
0	5	1.00	0.38	0.45	Brittle	Particulate
0	10	1.94	1.04	1.12	Brittle	–[a]
0	15	–	–	1.20	Ductile	Phase inversion
5	0	0.77	0.12	0.13	Brittle	Homogeneous
5	5	–	–	0.48	Ductile	Phase inversion
5	10	–	–	1.15	Ductile	Phase inversion
10	0	0.83	0.15	0.17	Brittle	Homogeneous
10	5	0.75	0.26	0.48	Brittle	Particulate
10	10	–	–	0.65	Ductile	Phase inversion
15	5	0.96	0.29	0.30	Brittle	Particulate
15	10	–	–	1.28	Ductile	Phase inversion
20	5	1.43	0.37	0.42	Brittle	Particulate
20	10	1.11	0.48	0.52	Brittle	Particulate
30	0	0.95	0.25	0.29	Brittle	Homogeneous

[a]Morphology could not be identified

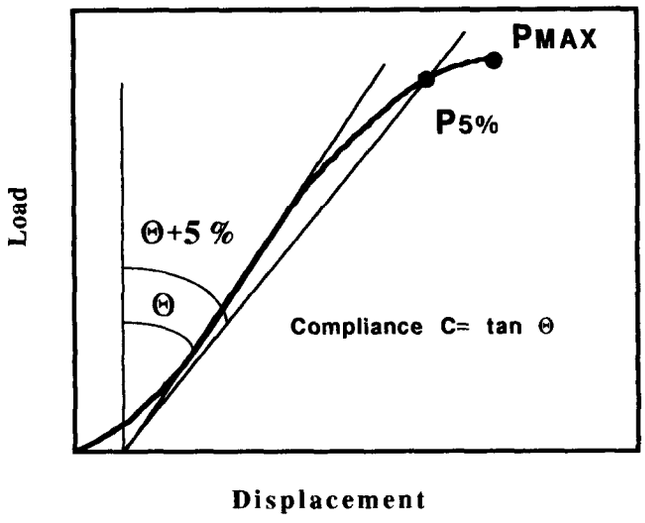

Figure 10 The determination of $P_{5\%}$ and compliance C in fracture toughness test

results in increased surface area, and the energy required to propagate such a crack increases. Quantitatively, the model may be stated as[16]:

$$\frac{K_c}{K_0} = \left(\frac{E_0}{E_c}(1 + 0.87V_f)\right)^{1/2} \quad (6)$$

where K_c is the fracture toughness of the modified epoxy, K_0 is the fracture toughness of the unmodified epoxy, E_c is the Young's modulus of the modified epoxy, E_0 is the Young's modulus of the unmodified epoxy, and V_f is the volume fraction of spheres. Given that the ratio of the Young's moduli is close to unity for the ternary system and the volume fraction of NBR rubber is no greater than 30%, then one may conclude that only a modest increase would be observed. Actually, on comparison of the K_{Ic} values of the binary systems and the ternary system, there seems to be no advantage in terms of fracture toughness on going to the ternary system.

In contrast, the ternary formulations that have the phase-inverted morphology as shown in *Figure 4* showed a non-linear load–displacement curve, which had broad peaks not well defined and the total displacement was significantly larger. With the formulations that showed ductile fracture behaviour, stress whitening was observed ahead of the initial notch when the load was applied above a certain level. The higher the load, the larger is the whitened region. The SEM micrograph in *Figure 9* shows the deformation of the polymer ahead of the crack tip in the crack opening direction. This deformation and drawing at the crack tip seems to dissipate the energy that is put into the material and make the material ductile. In those formulations, fracture toughness was improved from brittle to ductile on going to the ternary system from binary systems. According to the test protocol of the European Structural Integrity Society[12], to stay in the linear elastic fracture mechanics (LEFM) condition, it is further specified that:

$$P_{max}/P_{5\%} < 1.1 \quad (7)$$

where P_{max} is the maximum load and $P_{5\%}$ is the load where the initial compliance $C + 5\%$ intersects the load curve, as shown in *Figure 10*. If $P_{max}/P_{5\%} > 1.1$, the LEFM test is valid and non-linear fracture mechanics, the J-integral, should be introduced. The characteristic parameter, J, was obtained using the multi-specimen R-curve method[13]. The R-curves for each formulation are illustrated in *Figure 11*. J_{Ic} was taken by extrapolation of J to the point at which the displacement was zero. In the earlier literature[17–20], J_{Ic} values were determined at the point of intersection of the R-curve and the blunting line $J = 2\Delta a\sigma_y$. In this work, as shown in *Figure 12*, the intersection of the R-curve and the blunting line is close to the extrapolation of the R-curve to the point at which Δa is zero. Therefore, the load at the extrapolation of the R-curve was determined to be J_{Ic}. For comparison of the J parameter with each formulation, J_{Ic} values were calculated for the formulations that exhibited brittle fracture behaviour at the maximum load, P_{max}, *versus* the relationship given by the following equation[17]:

$$J = \frac{2U_{max}}{B(W - a)} \quad (8)$$

This was done because of difficulty in controlling Δa when $dJ/d(\Delta a)$ was small. The use of equation (8) was justified since no evidence of ductile tearing was visible on the fracture surfaces of these specimens, which were unloaded just prior to attainment of the maximum load.

Table 2 summarizes J_{Ic} values obtained by the procedure mentioned above. By the addition of NBR to PES/epoxy blend, the fracture behaviour changes from brittle to ductile and the J_{Ic} value increases dramatically below 15 phr of PES loading. Viscosity limitation did not permit the preparation of samples containing greater than 15 phr NBR. The blend containing more than 20 phr PES did not change its fracture behaviour on addition of NBR.

D.m.t.a. analysis

To determine the T_g of each phase and how the bulk properties of the matrix change with temperature, d.m.t.a. analysis was carried out. Representative curves illustrating the storage modulus and tan δ, as a function of temperature, of the four morphologically distinct formulations are shown in *Figures 13* and *14*. *Figure 13* illustrates the curves obtained from the binary system: one set is for 10 phr NBR-modified binary epoxy, which has particulate morphology, and the other set is for 5 phr PES-modified epoxy, which has no morphological features in the fracture surface. *Figure 14* illustrates the curves of the ternary system: one set is obtained from 10 phr NBR- and 15 phr PES-modified ternary blend, which has phase-inverted morphology, and the other set is from 5 phr PES- and 10 phr NBR-modified ternary blend, which has NBR-rich particulate morphology. The neat epoxy resin cured with DDS was also measured and the T_g was determined at 197°C from the peak of tan δ.

The NBR-modified binary system exhibits two glass transition values. The peak on the tan δ curve in the low-temperature region corresponds to the T_g of NBR-rich phase and the other one is the T_g of the epoxy-rich matrix phase. By addition of NBR, the T_g of the matrix decreases dramatically as listed in *Table 3*. In the PES-modified binary formulations, the T_g of the matrix did not decrease so much as for the NBR-modified binary system, and no other peaks were exhibited. As shown in *Figure 14*, the ternary systems showed two types of dynamic mechanical properties with distinct morphological states. The 10 phr NBR- and 15 phr

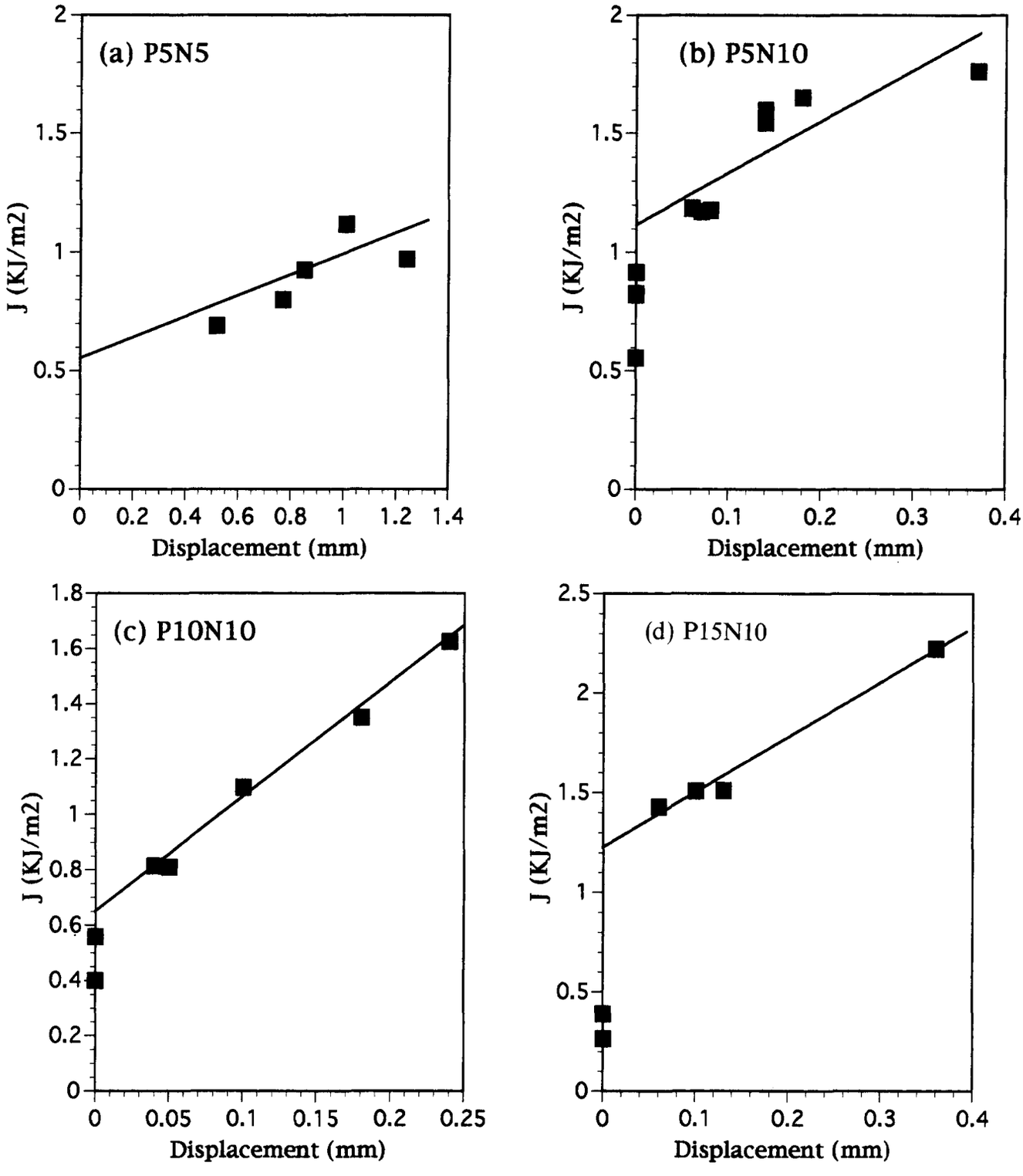

Figure 11 *J*-integral curves for epoxy/PES/NBR ternary blends: (a) P5N5; (b) P5N10; (c) P10N10; (d) P15N10

PES-modified ternary blend exhibits a large drop in the storage modulus at the T_g of the NBR-rich phase, and a third peak was present on the shoulder of the tan δ peak, which was assigned to epoxy-rich phase. The 5 phr NBR- and 10 phr PES-modified ternary blend exhibits two peaks on the tan δ curve, which were assigned to NBR-rich particles and epoxy-rich matrix respectively. In *Figure 15*, the T_g of the epoxy-rich phase determined by tan δ curve was plotted against the loading level of PES. With increase of PES loading level, the T_g increases and finally reaches the level of the neat epoxy's T_g.

The dynamic mechanical behaviour of these formulations is also explained by the respective morphologies of each formulation. The PES-modified binary system exhibited dynamic mechanical behaviour similar to that of the neat epoxy resin. Only one glass transition was observed on the tan δ curve, suggesting that no phase separation has occurred during the curing process.

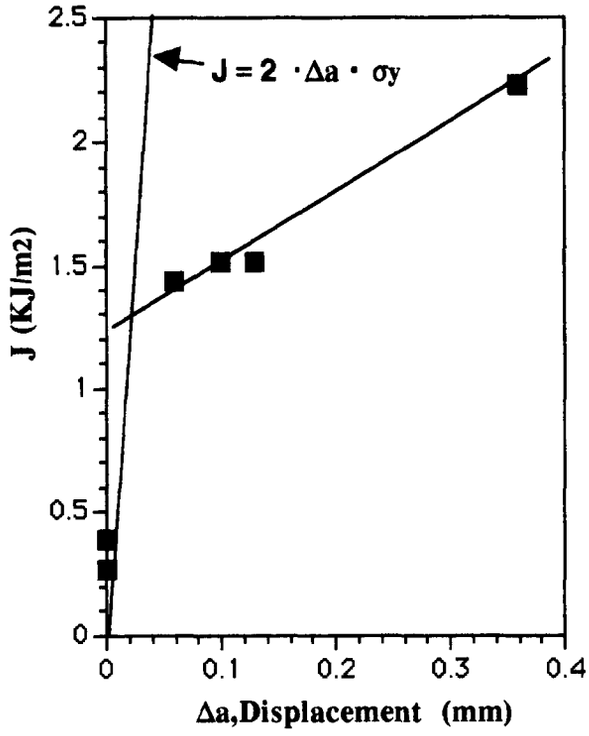

Figure 12 J-integral curves of N5P5 with blunting line ($J = 2\Delta a\sigma_y$)

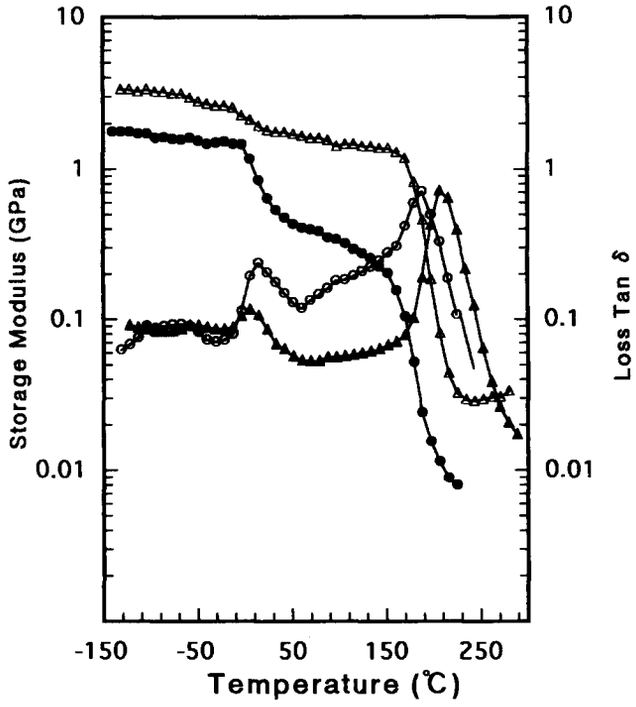

Figure 14 D.m.t.a. data of the ternary system: (●, ○) storage modulus and loss tan δ of 10 phr PES- and 15 phr NBR-modified ternary blend; (△, ▲) storage modulus and loss tan δ of 10 phr PES- and 5 phr NBR-modified ternary blend

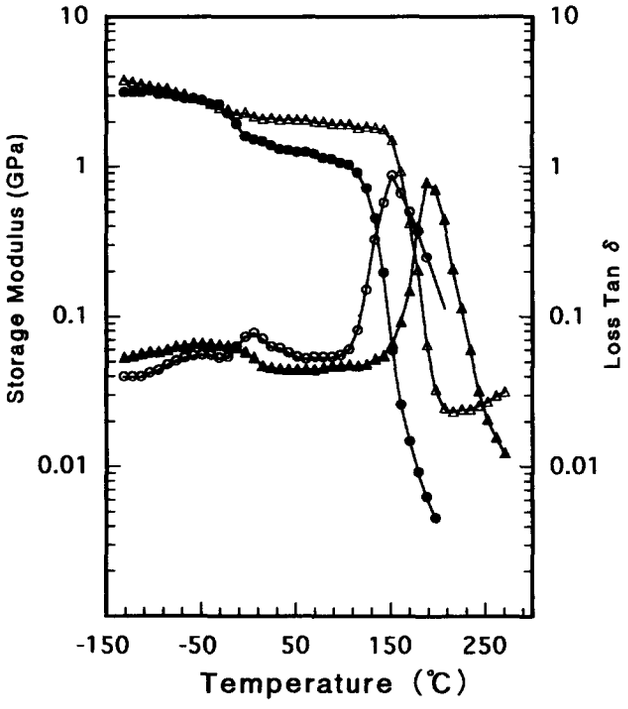

Figure 13 D.m.t.a. data of the binary systems: (●, ○) storage modulus and loss tan δ of 5 phr PES-modified binary blend; (△, ▲) storage modulus and loss tan δ of 10 phr NBR-modified binary blend

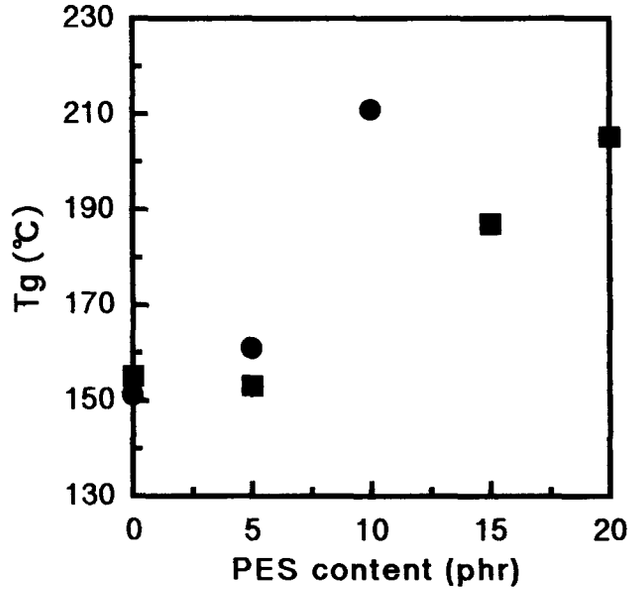

Figure 15 Effect of PES on T_g of epoxy-rich phase obtained from d.m.t.a. analysis: (●) 5 phr NBR; (■) 10 phr NBR

Within our formulation study of the PES-modified binary system (P5, P10 and P30), as listed in *Table 1*, all PES-modified binary formulations exhibited no surface features in the fracture test as shown in the SEM micrograph of P30 in *Figure 2*, and all the cured blends were transparent. It can therefore be thought that the cured blend is homogeneous and PES is miscible with the epoxy within the load range below 30 phr. With all ternary formulations, which have phase-inverted morphology as shown in *Figure 14*, a large drop in the storage modulus when the T_g of NBR was passed was observed. This suggests that the NBR-rich phase formed a continuous phase. A third peak on the shoulder of the peak of the epoxy-rich phase on tan δ was also detectable with these systems. With the morphological observation, this peak corresponds to small particles that exist around the epoxy-rich phase as shown in *Figure 5*. Another type of ternary formulation, which has particulate

Table 3 Glass transition temperature obtained from tan δ trace in d.m.t.a. analysis

Designation	T_g (°C) NBR	T_g (°C) Epoxy	Morphology
Epoxy	–	197	Homogeneous
N5	−17	151	Particulate
N10	1	155	–[a]
P5	–	189	Homogeneous
P5N5	15	161	Phase inversion
P5N10	17	153	Phase inversion
P10N5	5	211	Particulate
P15N10	19	187	Phase inversion
P20N10	3	205	Particulate

[a]Morphology could not be identified

morphology, exhibited similar dynamic mechanical behaviour to that of the NBR-modified binary system. There are two peaks on the tan δ curve corresponding to the T_g of NBR-rich phase and epoxy/PES matrix respectively. Compared with the NBR-modified binary system, the T_g of the NBR-rich phase is slightly greater in the ternary systems as listed in *Table 3*. This implies that in the ternary system the NBR-rich phase traps a certain amount of PES and epoxy.

Figure 15 shows the effect of PES on the T_g of the epoxy phase: there is a jump in T_g when the PES loading increases from 5 to 10 phr in the ternary system. One of the factors that could account in part for the increase of T_g is its relative melt viscosity. The higher loading level of PES exhibited greater viscosity and this increase may hinder phase separation, trap slightly more PES in the epoxy phase, and cause the high T_g of the epoxy phase. On the other hand, the T_g of the NBR-rich phase is little affected by the load of PES but depends on the morphology type of the formulations. The formulations having phase-inverted morphology show higher T_g of the NBR-rich phase than those having particulate morphology. This indicates that the NBR-rich phase in phase-inverted morphology includes more of the epoxy and PES.

CONCLUSION

In conclusion, it has been found that the incorporation of NBR/PES into a commercial high-performance epoxy/amine system can improve the fracture toughness from brittle to ductile. The NBR/PES-modified ternary systems have shown two distinct morphological states with mechanical and morphological properties unique to each. One consists of an NBR-rich matrix with epoxy-rich particles and PES-rich particles around the epoxy particles; the other consists of a PES/epoxy homogeneous matrix with NBR-rich particles that aggregate with each other to form large domains. As listed in *Table 2*, the addition of some NBR to the PES/epoxy single-phase system leads to phase inversion. This morphology creates a continuous rubber matrix, which allows deformation of the material at the crack front to absorb a large amount of energy prior to catastrophic failure of the material. The morphology in the ternary system depends on the combination of the loading level of NBR and PES. There seems to be a tendency that the higher the PES loading level, the more NBR is needed to obtain a phase-inverted morphology. Unfortunately, viscosity limitation did not permit the further loading of both PES and NBR, and hence it has not been possible to determine a direct morphology–loading level relationship, and further work is required.

The glass transition temperature of the ternary system increases with the loading of PES and finally reaches the unmodified epoxy's T_g when the PES loading level is more than 15 phr. Higher loading level of PES causes increased viscosity, which hinders phase separation and traps more PES in the epoxy-rich phase, and hence the high T_g of the epoxy phase can be achieved.

The results from this work have demonstrated that the modification of epoxy resin with a combination of rubber and thermoplastic is a promising toughening technique of brittle epoxy resin with minimal loss in thermal properties.

ACKNOWLEDGEMENTS

The authors wish to thank Dr Mitushashi and Mr Tsutusmi for carrying out the energy-dispersive spectroscopy and sulfur mapping experiments. Also, the help of Dr Nakayama during the d.m.t.a. analysis is gratefully acknowledged.

REFERENCES

1 Sue, H. I., Garcia-Meitin, E. I. and Pickleman, D. M. in 'Elastomer Technology Handbook' (Ed. N. P. Chermizinoff), CRC Press, Boca Raton, FL, 1993, Ch. 18, p. 661
2 Sultan, J. N., Liable, R. C. and McGarry, F. J. *Polym. Symp.* 1971, **16**, 127
3 Bucknall, C. B. and Partridge, I. K. *Polymer* 1983, **24**, 639
4 Bennett, G. S., Farris, R. J. and Thompson, S. A. *Polymer* 1991, **32**, 1633
5 Carfagra, C., Nicolais, L., Amendora, E., Carfagna, C. Jr and Filippov, A. G. *J. Appl. Polym. Sci.* 1992, **44**, 1465
6 McGrail, P. T. and Street, A. C. *Makromol. Chem., Macromol. Symp.* 1992, **64**, 75
7 Qipeng, G. *Polymer* 1993, **34**, 70
8 Gomez, C. M. and Bucknall, C. B. *Polymer* 1993, **34**, 2111
9 Pearson, R. A. and Yee, A. F. *J. Appl. Polym. Sci.* 1993, **48**, 1051
10 Pearson, R. A. and Yee, A. F. *Polymer* 1993, **34**, 3658
11 Li, S. J., Zhou, L. G. and Chen, Y. *J. Mater. Sci., Pure Appl. Chem.* (*A*) 1992, **29** (8), 609
12 Williams, J. G. and Cawood, M. J. European Structural Integrity Society, *Polym. Testing*, 1990, **9**, 15
13 Rice, J. G., Paris, P. C. and Merkle, J. G. ASTM STP 536, 1974
14 Bramuzzo, M. *Polym. Eng. Sci.* 1989, **29**, 1077
15 Wilkinson, S. P., Ward, T. C. and McGrath, J. E. *Polymer* 1993, **34**, 870
16 Farber, K. T. and Evans, A. G. *Acta Met.* 1983, **31**, 565
17 Hashemi, S. and Williams, J. G. *Polymer* 1986, **27**, 384
18 Narisawa, I. *Polym. Eng. Sci.* 1987, **27**, 41
19 Narisawa, I. and Takemori, M. T. *Polym. Eng. Sci.* 1989, **29**, 671
20 Zhang, M. J., Zhi, F. X. and Su, X. R. *Polym. Eng. Sci.* 1989, **29**, 1142